European Journal of Radiology 116 (2019) 34–40

Contents lists available at ScienceDirect

European Journal of Radiology

journal homepage: www.elsevier.com/locate/ejrad

Utilization of virtual non-contrast images derived from dual-energy CT in evaluation of biliary stone disease: Virtual non-contrast image can replace true non-contrast image regarding biliary stone detection

Jae Seok Bae[a,b], Dong Ho Lee[a,b,*], Ijin Joo[a,b], Sun Kyung Jeon[a], Joon Koo Han[a,b,c]

[a] Department of Radiology, Seoul National University Hospital, 101 Daehak-ro, Jongno-gu, Seoul, 03080, Republic of Korea
[b] Department of Radiology, Seoul National University College of Medicine, 103 Daehak-ro, Jongno-gu, Seoul, 03080, Republic of Korea
[c] Institute of Radiation Medicine, Seoul National University Medical Research Center, 103 Daehak-ro, Jongno-gu, Seoul, 03080, Republic of Korea

ARTICLE INFO

Keywords:
Dual-energy computed tomography
Contrast media
Cholelithiasis
Choledocholithiasis

ABSTRACT

Objectives: To compare the virtual non-contrast (VNC) images acquired through dual-energy computed tomography (DECT) with the true non-contrast (TNC) images in the detection of biliary stones and to calculate dose reduction by replacing TNC images with VNC images.

Methods: Between March 2017 and April 2018, we retrospectively enrolled 75 patients with suspicious biliary disease who underwent dual-source DECT and surgery and/or endoscopic intervention within 2 months from the CT. Biliary stones were present in 45 patients. The sensitivity and specificity for detecting gallstone and common bile duct (CBD) stone were compared between the VNC and TNC using McNemar test. In addition, the possible reduction in radiation dose was calculated.

Results: In our study, 37 patients had gallstones, 2 had CBD stones, and 6 had both gallstone and CBD stones. For detection of gallstones, the sensitivity and specificity were 90.7% (39/43) and 87.5% (28/32), respectively, for the TNC images, and 88.4% (38/43) and 90.6% (29/32), respectively, for the VNC images. With respect to CBD stones, the sensitivity and specificity were 87.5% (7/8) and 98.5% (66/67), respectively, for the TNC images, and 75.0% (6/8) and 100% (67/67), respectively, for the VNC images. There was no significant difference in the sensitivity and specificity between each image set ($P > 0.05$). The radiation dose reduction of 22.4 ± 1.3% is expected by omitting TNC images.

Conclusions: The VNC images derived from DECT were comparable to the TNC images for the detection of biliary stones and may replace the TNC images to reduce radiation dose.

1. Introduction

Cholelithiasis is a major health burden, with an escalating prevalence rate of 10–20% in the global adult population [1]. More than 20% of patients with cholelithiasis develop symptoms and complications including acute cholecystitis [1], and more than 750,000 cholecystectomies are performed annually in the US [2]. Moreover, concomitant common bile duct (CBD) stones are found in 10–20% of patients undergoing cholecystectomy for gallstones [3]. Because these residual stones can cause substantial morbidity such as cholangitis or pancreatitis, detection of the CBD stones before cholecystectomy is critical: detection of CBD stones enables selective endoscopic stone removal in those patients [3]. Thus, accurate preoperative diagnosis of patients with CBD stones as well as gallstones is important.

Ultrasound, magnetic resonance cholangiopancreatography (MRCP), endoscopic retrograde cholangiopancreatography (ERCP), or CT can be used to assess patients with suspected biliary stones. Ultrasound is a noninvasive tool, which has high sensitivity (98%) and specificity (93.5–97.7%) for the detection of gallstones [4]. However, the sensitivity of ultrasound for detection of CBD stones is low (25%) due to adjacent-bowel gas shadow [5]. For evaluation of CBD stones, ERCP and MRCP are widely utilized. Nevertheless, ERCP can be misleading due to the presence of air bubbles in the CBD or effect of the injection rate and concentration of contrast material [6]; in addition,

Abbreviations: DECT, dual-energy computed tomography; SECT, single-energy computed tomography; VNC, virtual non-contrast; TNC, true non-contrast; CBD, common bile duct; MRCP, magnetic resonance cholangiopancreatography; ERCP, endoscopic retrograde cholangiopancreatography; FOV, field of view; HU, Hounsfield unit; DLP, dose-length product

* Corresponding author at: Department of Radiology, Seoul National University Hospital, 101 Daehak-ro, Jongno-gu, Seoul, 03080, Republic of Korea.
E-mail address: dhlee.rad@gmail.com (D.H. Lee).

https://doi.org/10.1016/j.ejrad.2019.04.008
Received 8 December 2018; Received in revised form 11 April 2019; Accepted 14 April 2019

ERCP is an invasive procedure and complications such as perforation or death can occur [7]. Meanwhile, MRCP has high sensitivity (89–100%) and specificity (83–100%) for the diagnosis of choledocholithiasis [8,9]. However, there are disadvantages of MRCP including high cost, susceptibility to motion artifacts, or claustrophobia [10,11]. Currently, CT is widely used for evaluating patients with biliary tract disease [12]. Despite radiation exposure and moderate sensitivity (72–88%) for the detection of choledocholithiasis [13–15], CT has the advantages of a large field of view (FOV), high patient tolerance, and low susceptibility to artifacts [12]. Therefore, CT could be performed for the preoperative evaluation of patients with gallstones (previously confirmed with US) to assess the presence of CBD stones and rule out biliary malignancy caused by cholelithiasis and/or choledocholithiasis [16].

Recently, dual-energy CT (DECT) has gained interest in the evaluation of biliary stone disease [17–24]. Current DECT scanners have the capability to simultaneously acquire two datasets with different X-ray energy spectra including low–kilovolt-peak (typically 80–100-kVp) and high–kilovolt-peak (typically 140–150-kVp) [12]. Various post-processing techniques can be used subsequently for the differentiation or quantification of materials with different X-ray absorption profiles [25]. Among the DECT post-processing methods, virtual non-contrast (VNC) images can be created by subtracting the iodine content from the contrast-enhanced DECT images. If VNC images could provide comparable diagnostic performance in detecting biliary stone disease to TNC, we might replace TNC with VNC, and consequently, reduce the radiation dose. Therefore, the purpose of this study was to compare the capability of the VNC images derived from DECT with that of the TNC images to detect gallstones and/or CBD stones, and to assess whether the TNC images can be replaced with VNC images for evaluating patients with biliary stone disease. We also aimed to calculate potential savings in radiation dose.

2. Materials and methods

2.1. Patients

This retrospective study was approved by our hospital's institutional review board and the requirement for informed consent was waived. From late March 2017 to April 2018, 2176 consecutive patients (1057 men, 1119 women; mean age, 62.9 ± 12.3 years; age range, 18–97 years) underwent biliary protocol CT using a DECT scanner in dual-energy mode in our hospital under clinical suspicion of biliary disease. The inclusion criteria were as follows: 1) The presence or absence of gallstone and/or CBD stone confirmed by surgery (n = 97) or endoscopy including endoscopic ultrasound (EUS) and/or ERCP (n = 11) and 2) interval between surgery or endoscopy and CT examination of within 2 months. The interval of 2 months was chosen because a too long time interval between CT and reference standards can decrease the reliability of CT finding because of possible change (e.g. migration of gallstone to the CBD or duodenum). However, applying a too short time interval between CT and reference standards would significantly decrease the number of eligible patients. Consequently, the interval of 2 months was chosen to balance the issue of reliability of CT findings and the possible sample size. The surgery/EUS/ERCP findings served as the reference standard for the presence of biliary stones. From among the 108 patients who met the inclusion criteria, we excluded nine patients who underwent biliary intervention such as percutaneous transhepatic biliary drainage. Thereafter, biliary stones were present in 69 patients and were absent in 30 patients. Among the 69 patients with biliary stones, we included 45 patients who were age- and sex-matched with those without biliary stones. Finally, 75 patients (34 men; mean age, 64.8 ± 9.4 years; age range, 48–90 years) were included in our study (Fig. 1). The indications for cholecystectomy are summarized in the Appendix AAppendix. The mean time interval between CT and surgery and/or ERCP was 16.1 ± 19.3 days (range, 1–60 days).

The DECT scanner in our hospital was operated in the single-energy CT (SECT) mode before late March 2017; hence, a control group for comparing the radiation dose between the DECT and SECT modes was feasible. From January 2017 to March 2017, we included all 167 consecutive patients (80 men; mean age, 64.3 ± 13.6 years; age range, 24–92 years) who underwent the same biliary protocol CT in the SECT mode through the same scanner as a control group for the radiation dose comparison.

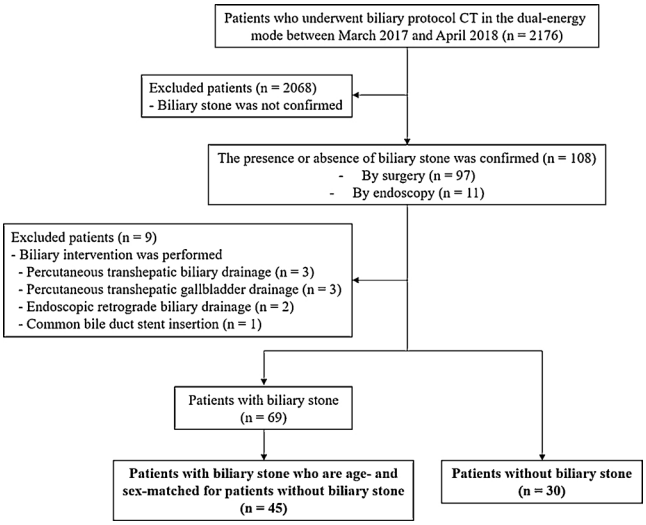

Fig. 1. Flow diagram of the study population.

2.2. CT image acquisition and post-processing

All CT scans were performed using a dual-source DECT scanner (SOMATOM Force; Siemens Healthineers, Forchheim, Germany). The gantry of the scanner comprised of two X-ray tubes-detector combinations at 95° angle; 384 slices were obtained (192 sections for each detector) and a flying focal spot was used. The FOVs were 50 cm and 35 cm for detector A and B, respectively. In our hospital, routine biliary CT protocol comprises precontrast, early arterial, late arterial, and portal venous phase images. The late arterial phase images were obtained in the DECT mode using 80-kVp and 250-mAs and 150-kVp and 125-mAs for the detectors A and B, respectively, and the other phase images were obtained in the SECT mode using 90-kVp and 180-mAs. We used the liver VNC setting to generate an iodine map which represents the iodine distribution per pixel in the dual-energy CT images. Subsequently, iodine was subtracted from the images and the VNC images were generated. Further information is provided in Appendix AAppendix.

2.3. Qualitative image analysis

For the purpose of detection of biliary stones on the TNC and VNC images, two radiologists (with 12 and 5 years' experience in abdominal imaging) who were blinded to the presence of biliary stones performed independent review on the 75 patients on the PACS workstation (Fig. 2). Default window levels of the TNC and VNC images were window width of 320 HU and 400 HU, respectively, and window level of 50 HU and 40 HU, respectively. However, the window width and level were modified at the reviewers' discretion. To minimize recall bias, all TNC and VNC images were assessed at an interval of 2 weeks. On each image set, the presence of stone in the gallbladder and CBD was evaluated. Combined presence of the stone and radiodensity was categorized on a 3-point scale (1, no stone; 2, radiolucent stone; and 3, radiopaque stone). Because calcified, radiopaque stones are relatively easily identified, whereas cholesterol stones that are slightly hypo- or isoattenuating to surrounding bile are often difficult to detect [13,22],

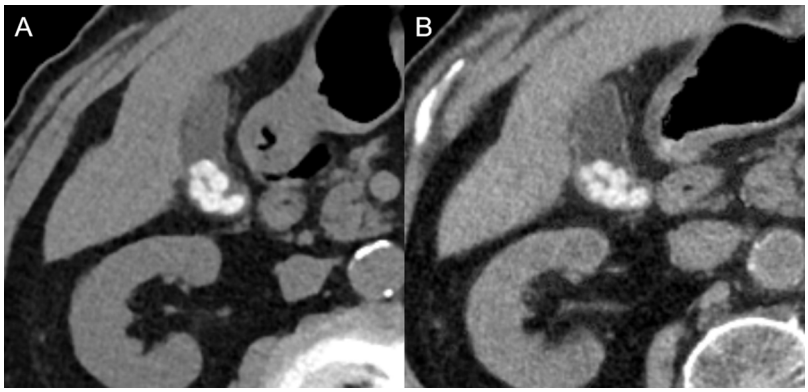

Fig. 2. Representative case of the TNC and VNC images. The patient is an 87-year-old man with gallstones. Both the TNC (A) and VNC (B) images depict multiple calcified gallstones. The mean attenuation values of the gallstones are 205.7 HU and 147.7 HU on the TNC and VNC images, respectively. In qualitative analysis, the reviewers' report indicates the presence of gallstones on both the TNC and VNC images.

stone radiodensity was classified into two categories of radiolucent and radiopaque based on the comparison between the stone and bile. If the stone appears hyperdense than the surrounding bile, the stone was considered as radiopaque, and if the stone appears hypodense than of the surrounding bile, the stone was regarded as radiolucent. After independent review, the two radiologists reached a consensus and disagreements were resolved through discussion with another radiologist (with 13 years' experience in abdominal imaging).

2.4. Quantitative image analysis

One radiologist (with 6 years' experience in abdominal imaging) performed objective measurements of the TNC and VNC image sets of all 75 patients on a picture archiving and communication system workstation (Infinitt PACS viewer, Infinitt, Seoul, Korea). The radiologist was informed of the presence of gallstones and/or CBD stones. In case of the presence of biliary stones, the mean attenuation values and size of stones was assessed. In case of the presence of multiple stones, the diameter of the largest stone was measured. If a patient had stones in both gallbladder and CBD, measurement was performed for the largest ones in each area. The size of the biliary stones was measured on the axial images of each image set and the maximum diameter was used [26,27]. To measure the mean and standard deviation of attenuation values of the stone, bile, and paraspinal muscle, three consecutive axial imaging planes were selected to obtain the maximum cross-sectional area of the biliary stone in each image set [17]. To measure the attenuation of the stone, the freehand region of interest (ROI) technique was used with ROIs drawn along the inner margin of the stone and the attenuation values obtained at the three imaging planes were averaged. In addition, contrast-to-noise ratio (CNR) of the stone-to-bile was calculated by subtracting the mean attenuation value of the bile from that of the stone and dividing it by the mean SD value of the paraspinal muscle, respectively [17].

2.5. Radiation dose analysis

The effective radiation dose was calculated by multiplying the dose-length product (DLP) by the conversion factor. The DLP was automatically shown in the patients' dose report, and the conversion factor for abdomen was 0.015 per the International Commission on Radiological Protection recommendation [28].

2.6. Statistical analysis

Paired or independent *t*-test was performed to compare variables between VNC and TNC images. The sensitivity and specificity for detection of biliary stone was determined based on the consensus of the two reviewers on each image set, and compared using McNemar test. Factors with $P < 0.05$ were considered statistically significant. Interobserver agreement for the presence of stone and qualitative analysis of the VNC images was assessed using weighted kappa statistics. The kappa value was interpreted as follows: < 0.2, poor; 0.21–0.40, fair; 0.41–0.60, moderate; 0.61–0.80, good; and 0.81–1.00, very good. Commercially available softwares (IBM Statistical Package for the Social Sciences (SPSS) for Windows, Version 22.0 (IBM Corp., Armonk, NY, USA) and MedCalc for Windows, version 18.6 (MedCalc Software, Ostend, Belgium)) were used for statistical analysis.

3. Results

3.1. Detection of biliary stone: standard reference

Among the 45 patients with biliary stones, 37 patients had only gallstones, six patients had both gallstones and CBD stones, and the other two patients had only CBD stones. The presence of 36 gallstones and one CBD stone was confirmed through surgery, and that of seven gallstones and seven CBD stones through EUS and/or ERCP. Altogether there were 43 confirmed gallstone cases and 8 confirmed CBD stone cases.

3.2. Qualitative analysis

For the purpose of detection of gallstones and CBD stones, both the sensitivity and specificity showed no significant differences between the TNC and VNC images ($P > 0.999$ for all) (Table 1). Interobserver agreement was very good for both the TNC and VNC images in the evaluation of gallstones (0.840 and 0.946, respectively) and CBD stones (0.934 and 0.819, respectively). The biliary stones moved to different positions in the VNC images compared to the TNC images in five patients; however, this movement showed no impact on the detection rate of the stones (Fig. 3).

There were eight cases which showed discrepancy in findings of the presence of stone between the TNC and VNC images including six

Table 1
Diagnostic Performance of the True and Virtual Non-Contrast Images in the Detection of Biliary Stones.

		True non-contrast	Virtual non-contrast	Difference*	*P* value
Gallstone	Sensitivity (%)	90.7 (39/43)	88.4 (38/43)	2.33 (-5.66, 6.86)	> 0.999
	Specificity (%)	87.5 (28/32)	90.6 (29/32)	−3.12 (-9.22, 7.61)	> 0.999
CBD stone	Sensitivity (%)	87.5 (7/8)	75.0 (6/8)	12.50 (-11.8, 12.50)	> 0.999
	Specificity (%)	98.5 (66/67)	100.0 (67/67)	−1.49 (-1.49, 1.42)	> 0.999

CBD = common bile duct.
* Number in parentheses are 95% confidence intervals.

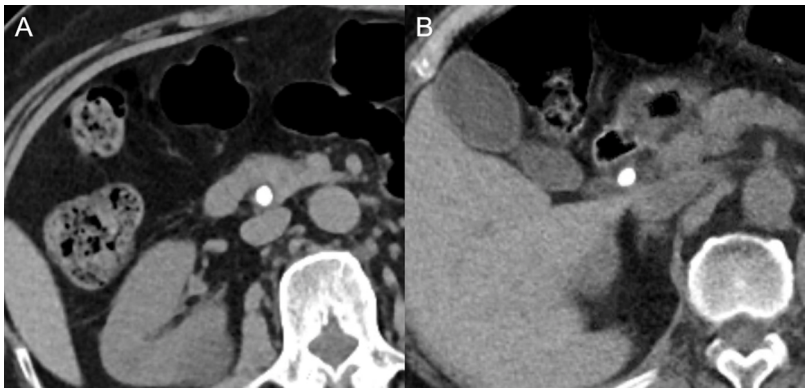

Fig. 3. Representative case showing movement of biliary stones on the VNC images compared with the TNC images. The patient is a 68-year-old woman with an 8-mm stone at the distal common bile duct on the TNC images (A). However, on the VNC images, the stone is located at the proximal common bile duct, near the insertion site of the cystic duct (B).

Table 2
Patients with Discrepancy in Findings of the Presence of Stone between the True and Virtual Non-Contrast Images.

	True non-contrast		Virtual non-contrast	
	False positive	False negative	False positive	False negative
Gallstone (n = 6)	2	1	1	2
CBD stone (n = 2)	1	0	0	1

CBD = common bile duct.

gallstones and two CBD stones (Table 2). In a case with FP result in the VNC image set, the presence of a small radiopaque stone was suspected on the VNC images, but not on the TNC images (Fig. 4). Surgery revealed the absence of stone or polyp in the gallbladder. Regarding the CBD stones, there was one FN case on the VNC images and none on the TNC images (Fig. 5) and one FP case on the TNC images and none on the VNC images. Information on the chemical composition of the gallstones with FP and FN results on the VNC image and all the CBD stones was not available through the pathology database search. In addition, in five patients, there was finding of radiolucent gallstones on the TNC images which were missed; whereas, on the VNC images, two of those gallstones were radiopaque and detected (Fig. 6). In the surgical specimen of the two radiopaque stones on the VNC images, pure cholesterol stone and black pigmented stone were visually identified. The mean attenuation value of the pure cholesterol stone was 23.70 HU and 53.58 HU on the TNC and VNC images, respectively. The patient showed mean attenuation value of the bile of 16.92 HU and 5.79 HU, respectively, yielding CNRs of -1.75 and 2.22 on the TNC and VNC images, respectively. There was no radiolucent CBD stone.

3.3. Quantitative analysis

Regarding the stone, we excluded the small stones of size < 5 mm (n = 7) due to difficulty in accurate measurement and quantitative analysis of biliary stone was performed in the remaining 38 patients. Both the gallstones and CBD stones had higher attenuation values on the TNC than the VNC images (Table 3). The size of the stone did not differ significantly between the TNC and VNC images. The CNRs of the stone-to-bile were significantly higher on the TNC than on the VNC images.

3.4. Radiation dose analysis

For estimation of the radiation dose, four and three patients were excluded from the DECT and SECT group respectively, because of repeated scanning due to insufficient coverage at portal phase. There were no differences in the patients' age, sex, or body mass index between the DECT and SECT groups. Despite difference in the effective dose at precontrast, early arterial, and portal phase between the DECT and SECT groups, the total effective dose for biliary protocol CT scan showed no significant difference (10.6 ± 3.5 and 10.2 ± 1.0 mSv, respectively) (P = 0.368) (Table 4). The effective dose for the TNC images in the DECT group was 2.4 ± 0.8 mSv. Therefore, the radiation dose may be reduced by replacement of TNC images with VNC images, thereby eliminating the need for acquisition of non-contrast scan; under such condition, the total effective dose for biliary protocol CT performed in our hospital would be decreased by 22.4 ± 1.3 (2.4/10.6)%.

4. Discussion

Our study showed that the VNC image derived from dual source DECT was comparable to the TNC image in effectiveness to detect biliary stones and may be considered as acceptable replacement for the TNC image. The sensitivity and specificity for detection of gallstones and CBD stones showed no significant difference between each image set. In particular, this is the first study that evaluated the specificity for the detection of CBD stones on the VNC images. Hence, the VNC images

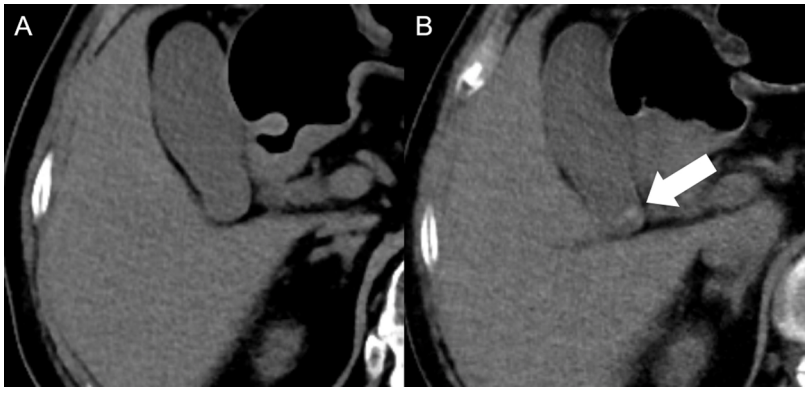

Fig. 4. Representative false-positive case of the VNC image. The patient is a 76-year-old woman with the true non-contrast image showing the absence of stone (A). However, on the VNC image, a subtle radiopaque lesion is observed at the proximal body of the gallbladder (arrow) on the VNC image (B). Cholecystectomy was performed and both the operative finding and surgical specimen reveal the absence of gallstone. In qualitative analysis, reviewers' report indicates the presence of gallstone on the VNC images alone.

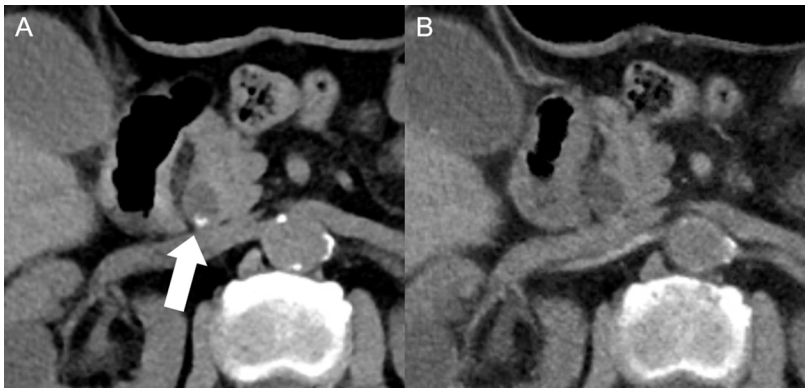

Fig. 5. Representative false-negative case of the VNC image in a 78-years-old male patient. (A) On the TNC image, a radiopaque stone is observed in the dependent portion of the CBD (arrow). (B) On the VNC image, there was no radiopaque stone along the CBD and gallbladder. In qualitative analysis, the reviewers' report indicates the presence of CBD stone on the TNC images alone. ERCP was performed before cholecystectomy and the distal CBD stone was removed (not shown).

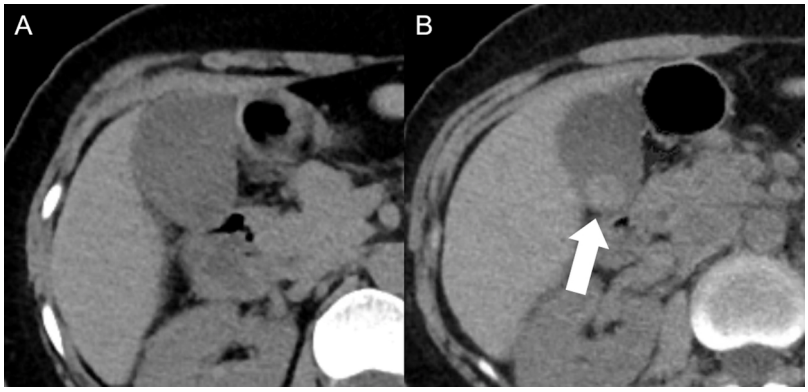

Fig. 6. The patient is a 49-year-old female patient with ill-defined presence of gallstone on the TNC image (A). In contrast, a radiopaque stone is observed in the dependent portion of the gallbladder (arrow) on the VNC image (B). Reviewers' report indicates the presence of a gallstone on the VNC images alone. In quantitative analysis, the mean attenuation values of the gallstone are 23.7 HU and 53.6 HU on the TNC and VNC images, respectively. In terms of the contrast-to-noise ratio of the stone-to-bile, -1.75 and 2.22 was obtained on the TNC and VNC images, respectively. Surgery revealed a 1.5-cm pure cholesterol stone in the surgical specimen.

Table 3
Quantitative Analysis of the True and Virtual Non-contrast Images.

Characteristics	True non-contrast	Virtual non-contrast	*P* value
Attenuation (HU)			
Stone			
Gallstone (n = 43)	354.68 ± 402.21	207.22 ± 204.30	**0.001**
CBD stone* (n = 8)	392.97 (86.06–1354.45)	220.44 (56.10–702.00)	**0.021**
Bile	18.03 ± 8.01	11.74 ± 12.13	< **0.001**
Stone size (mm)	13.57 ± 6.00	12.43 ± 5.98	0.102
Contrast-to-noise ratio (stone-to-bile)	31.49 ± 38.46	16.76 ± 20.05	< **0.001**

Note. HU = Hounsfield unit, CBD = common bile duct.
* number in parenthesis is range. Other numerical values are mean ± standard deviation.

Table 4
Clinical Characteristics and Effective Radiation Doses in the Patients Who Underwent Biliary Protocol CT under Dual-Energy Mode and Single-Energy Mode.

	Dual-energy mode (n = 71)	Single-energy mode (n = 164)	*P* value
Age	64.8 ± 9.4	64.4 ± 13.8	0.800
Sex (male : female)	31 : 40	80 : 84	0.471
Body mass index (kg/m^2)	24.1 ± 3.2	23.3 ± 4.2	0.168
Effective dose (mSv)			
Precontrast phase	2.35 ± 0.82	2.66 ± 0.88	**0.012**
Early arterial phase	2.36 ± 0.81	2.07 ± 0.68	**0.005**
Late arterial phase	2.06 ± 0.72	2.05 ± 0.65	0.933
Portal phase	3.70 ± 1.18	3.31 ± 0.97	**0.008**
Total	10.58 ± 3.47	10.17 ± 3.06	0.368

may eliminate the need for acquisition of TNC images, especially for the evaluation of biliary stone, thereby reducing the radiation exposure in patients undergoing TNC imaging which accounts for 22.4% of the total radiation dose in the biliary protocol CT.

In the biliary-pancreas protocol CT, one of the most important roles of TNC imaging is the evaluation and detection of biliary stones such as gallbladder and/or CBD stones by enabling differentiation between the enhancing bile duct wall and biliary stones [14,29]. Although previous studies have assessed the feasibility of using the VNC as replacement for TNC images in patients with biliary stones, those studies did not include a control group without stones and the diagnostic performance of VNC in detecting CBD stone compared to that of TNC has not been fully evaluated [17,20]. In our study, the diagnostic performance of the VNC images to detect biliary stones was similar to that of the TNC images and was comparable to the results of recent studies. Regarding the detection of gallstones on VNC images, Lee et al reported sensitivity and specificity of 76–77% and 84–88%, respectively [20]; in the same study, the sensitivity and specificity of the TNC images were 79–80% and 91–95%, respectively. Although there were discrepancies between the TNC and VNC diagnoses (n = 8), the TNC and VNC equally yielded false diagnosis in four cases each and there was no significant difference in diagnostic performance for detection of biliary stone using both techniques.

The VNC images helped detection of 40% (2 of 5) radiolucent gallbladder stones which were not detected on the TNC images in our study (Fig. 5). This result is in concordance with that of a previous study reporting a higher CNR value in cholesterol stones on the VNC than that on the TNC images [20]. This phenomenon may be explained by the high HU value in cholesterol stones at 150-kVp [30]. Because our VNC images was constructed as weighted average images from 40% images of 150-kVp and 60% of 80-kVp, the mean attenuation value in the cholesterol stones would be higher on the VNC images than that on the TNC images obtained at 90-kVp. Therefore, the VNC images may be advantageous for detection of radiolucent stones than the TNC images.

The VNC images could reduce the radiation dose by eliminating the need to acquire the TNC images because the VNC images provided comparable diagnostic capability in detecting biliary stones compared to the TNC images. The expected amount of dose reduction was 22.4 ± 1.3% compared with that of conventional biliary protocol CT in our institution, which is lower than the value reported by previous studies of range from 56.4%–34.9% [11,26]. This discrepancy is probably due to the difference in CT protocols: We used quadruple-phase CT, whereas triple-phase CT or CT urography was utilized in the previous studies. In contrast, our result corroborates those reported by De Cecco et al of mean dose reduction of 21.1% achieved by omitting the TNC images [27]. This variation in the amount of radiation exposure from the acquisition of the TNC images may be due to optimization of the CT parameters or scanning protocols. However, based on our result and those previously reported, at least 20% of total radiation dose reduction could be achieved by replacing the TNC images with the VNC images.

Movement of the biliary stones to different positions was observed in five patients on the VNC images compared to the TNC images. In our study, the VNC images were generated from late arterial phase images obtained after injection of contrast material. Thus, lengthened time of the CT examination and allergy to the contrast media could have caused involuntary movement of the patients. However, the reviewers diagnosed the presence of biliary stones accurately in those patients showing the movement of stones without diagnostic impairment.

Our study has a few limitations. First, this single center retrospective study has a certain degree of selection bias. Second, the results were obtained using a dual-source DECT scanner from a single vendor, and may not be generalized to the VNC images acquired through DECT scanners based on different techniques such as fast-kVp switching or dual-layer detector spectral CT. Third, analysis of the composition of biliary stones was not possible in all participating patients due to the study's retrospective design. In addition, the number of included patients with CBD stones was small (n = 8). Further studies including larger number of patients with CBD stones are needed to confirm the role of VNC images in evaluation of patients with CBD stones. Regarding the selection of patients with biliary stones matched to those without stones, we chose the patients who were age- and sex-matched and this might be a source of bias. We also did not evaluate the role of VNC images with respect to the baseline images for determining the presence of enhancement. Finally, we did not compare the diagnostic performance of the combined TNC and contrast-enhanced images with that of the combined VNC and contrast-enhanced images. However, in our hospitals' routine clinical practice, non-contrast images play a crucial role in the detection of biliary stones as for urinary stones; hence, it is likely that comparing the TNC and VNC images alone would be sufficient to evaluate the diagnostic value of imaging in patients with biliary stones.

5. Conclusion

The VNC images derived from a dual-source DECT scanner demonstrated similar diagnostic performance to that of the TNC images in the evaluation of biliary stones with high interobserver agreement. The VNC images showed potential for use as an alternate to the TNC images with reduction in the radiation dose in patients with biliary stones.

Appendix A

Indications for Cholecystectomy

Surgery was performed in 66 patients for the following reasons: chronic cholecystitis (n = 41), pancreatic ductal adenocarcinoma (n = 6), gallbladder adenocarcinoma (n = 4), intracholecystic papillary or tubopapillary neoplasm (n = 4), intraductal papillary mucinous neoplasm of the pancreas (n = 4), metastatic adenocarcinoma in the liver from the rectum (n = 2), common bile duct cancer (n = 2), intrahepatic cholangiocarcinoma (n = 1), acute gangrenous cholecystitis (n = 1), and pancreatic neuroendocrine tumor (n = 1). The types of surgery were as follows: cholecystectomy (n = 47), pylorus-preserving distal pancreatectomy (n = 6), Whipple's operation (n = 5), cholecystectomy with hemihepatectomy (n = 3), cholecystectomy with bile duct resection (n = 2), extended cholecystectomy (n = 2), and cholecystectomy with distal pancreatectomy (n = 1).

CT Image Acquisition and Post-Processing

After obtaining the precontrast images, iobitridol (Xenetix 350; Schering Korea, Seoul, Korea) at a dose of 1.5 mL/kg was injected at a rate of 3.0–4.0 mL/s using a power injector (Envision CT; Medrad, Pittsburgh, PA, USA), followed by injection of 30–40 mL of normal saline. Using the bolus-tracking method (CARE Bolus; Siemens Healthineers, Forchheim, Germany), early arterial phase images were acquired automatically at 7 s after achievement of attenuation of 100 Hounsfield unit (HU) in the descending aorta. Subsequently, late arterial phase and portal venous phase images were obtained immediately after the early arterial phase and 70 s after the administration of contrast agent, respectively. The tube currents were adjusted in real-time by automatic dose modulation provided by the manufacturer (Care Dose4D; Siemens Healthineers, Forchheim, Germany) to maintain the optimal level of image noise. With regard to biliary protocol CT, non-contrast, early arterial, and portal venous phase images were obtained using 90-kVp tube voltage (collimation, 192 × 0.6 mm; rotation time, 0.5 s; pitch, 0.6; and kernel Br40) and 180-mAs tube current–time product. With regard to dual-energy mode, the late arterial phase images were obtained using 80-kVp and 250 mAs and 150-kVp and 125 mAs for the detectors A and B, respectively, using the following parameters: Collimation, 128 × 0.6 mm; rotation time, 0.5 s; pitch, 0.6; and kernel Br40; with regard to single-energy mode used in the control group, the images at all phases were acquired using 90-kVp tube energy (collimation, 192 × 0.6 mm; rotation time, 0.5 s; pitch, 0.6; and kernel Br40) and 180-mAs tube current–time product.

Dual-energy late arterial phase images were obtained as weighted average images from the two detectors with ratio of 0.6 (40% 150-kVp and 60% 80-kVp), and transferred to a dedicated dual-energy post-processing workstation (Syngo.via, Client 4.1, Siemens Healthineers, Forchheim, Germany). We used the liver VNC setting to generate an iodine map which represents the iodine distribution per pixel in the CT images. Subsequently, iodine was subtracted from the images and the VNC images were generated. Three-material decomposition algorithm based on the assumption that fat, soft tissue, and iodine constitutes each CT voxel was used for the calculation [26]. For the purpose of the liver VNC applications, 60 HU and 56 HU were used as the standard soft-tissue attenuation and -110 HU and -84 HU were used as the standard fat attenuation at 80- and 150-kVp, respectively. The relative contrast material enhancement factor was set as 3.46, and the resolution enhancement, organ-contour enhancement, and beam-hardening correction were used. Axial images of the TNC and VNC were reconstructed using 3-mm-thick sections and 2-mm increments.

References

[1] F. Lammert, K. Gurusamy, C.W. Ko, J.F. Miquel, N. Mendez-Sanchez, P. Portincasa, K.J. van Erpecum, C.J. van Laarhoven, D.Q. Wang, Gallstones, Nat. Rev. Dis. Primers 2 (2016) 16024.
[2] L.M. Stinton, R.P. Myers, E.A. Shaffer, Epidemiology of gallstones, Gastroenterol. Clin. North Am. 39 (2) (2010) 157–169 vii..
[3] B.V. Dasari, C.J. Tan, K.S. Gurusamy, D.J. Martin, G. Kirk, L. McKie, T. Diamond, M.A. Taylor, Surgical versus endoscopic treatment of bile duct stones, Cochrane Database Syst. Rev. 12 (2013) CD003327.
[4] P.L. Cooperberg, H.J. Burhenne, Real-time ultrasonography. Diagnostic technique of choice in calculous gallbladder disease, N. Engl. J. Med. 302 (23) (1980) 1277–1279.
[5] B.H. Gross, L.P. Harter, R.M. Gore, P.W. Callen, R.A. Filly, H.A. Shapiro,

H.I. Goldberg, Ultrasonic evaluation of common bile duct stones: prospective comparison with endoscopic retrograde cholangiopancreatography, Radiology 146 (2) (1983) 471–474.
[6] C.M. Wilcox, Endoscopic examination with the duodenoscope at ERCP: frequency of lesions and accuracy of detection, Gastrointest. Endosc. 55 (4) (2002) 538–542.
[7] A.S.o.P. Committee, M.A. Anderson, L. Fisher, R. Jain, J.A. Evans, V. Appalaneni, T. Ben-Menachem, B.D. Cash, G.A. Decker, D.S. Early, R.D. Fanelli, D.A. Fisher, N. Fukami, J.H. Hwang, S.O. Ikenberry, T.L. Jue, K.M. Khan, M.L. Krinsky, P.M. Malpas, J.T. Maple, R.N. Sharaf, A.K. Shergill, J.A. Dominitz, Complications of ERCP, Gastrointest. Endosc. 75 (3) (2012) 467–473.
[8] K. Hekimoglu, Y. Ustundag, A. Dusak, Z. Erdem, B. Karademir, S. Aydemir, S. Gundogdu, MRCP vs. ERCP in the evaluation of biliary pathologies: review of current literature, J. Dig. Dis. 9 (3) (2008) 162–169.
[9] J. Romagnuolo, M. Bardou, E. Rahme, L. Joseph, C. Reinhold, A.N. Barkun, Magnetic resonance cholangiopancreatography: a meta-analysis of test performance in suspected biliary disease, Ann. Intern. Med. 139 (7) (2003) 547–557.
[10] C.W. Kim, J.H. Chang, Y.S. Lim, T.H. Kim, I.S. Lee, S.W. Han, Common bile duct stones on multidetector computed tomography: attenuation patterns and detectability, World J. Gastroenterol. 19 (11) (2013) 1788–1796.
[11] S.T. Schindera, R.C. Nelson, E.K. Paulson, D.M. DeLong, E.M. Merkle, Assessment of the optimal temporal window for intravenous CT cholangiography, Eur. Radiol. 17 (10) (2007) 2531–2537.
[12] B.M. Yeh, P.S. Liu, J.A. Soto, C.A. Corvera, H.K. Hussain, MR imaging and CT of the biliary tract, Radiographics 29 (6) (2009) 1669–1688.
[13] S.W. Anderson, B.C. Lucey, J.C. Varghese, J.A. Soto, Accuracy of MDCT in the diagnosis of choledocholithiasis, AJR Am. J. Roentgenol. 187 (1) (2006) 174–180.
[14] J.D. Neitlich, M. Topazian, R.C. Smith, A. Gupta, M.I. Burrell, A.T. Rosenfield, Detection of choledocholithiasis: comparison of unenhanced helical CT and endoscopic retrograde cholangiopancreatography, Radiology 203 (3) (1997) 753–757.
[15] S.W. Anderson, E. Rho, J.A. Soto, Detection of biliary duct narrowing and choledocholithiasis: accuracy of portal venous phase multidetector CT, Radiology 247 (2) (2008) 418–427.
[16] T.M. Welzel, B.I. Graubard, H.B. El-Serag, Y.H. Shaib, A.W. Hsing, J.A. Davila, K.A. McGlynn, Risk factors for intrahepatic and extrahepatic cholangiocarcinoma in the United States: a population-based case-control study, Clin. Gastroenterol. Hepatol. 5 (10) (2007) 1221–1228.
[17] J.E. Kim, J.M. Lee, J.H. Baek, J.K. Han, B.I. Choi, Initial assessment of dual-energy CT in patients with gallstones or bile duct stones: can virtual nonenhanced images replace true nonenhanced images? AJR Am. J. Roentgenol. 198 (4) (2012) 817–824.
[18] H. Li, D. He, Q. Lao, X. Chen, M. Liu, B. Yin, K. Zhao, R. Wang, L. Chen, Clinical value of spectral CT in diagnosis of negative gallstones and common bile duct stones, Abdom. Imaging 40 (6) (2015) 1587–1594.
[19] A.L. Chen, A.L. Liu, S. Wang, J.H. Liu, Y. Ju, M.Y. Sun, Y.J. Liu, Detection of gallbladder stones by dual-energy spectral computed tomography imaging, World J. Gastroenterol. 21 (34) (2015) 9993–9998.
[20] H.A. Lee, Y.H. Lee, K.H. Yoon, D.H. Bang, D.E. Park, Comparison of virtual unenhanced images derived from dual-energy CT with true unenhanced images in evaluation of gallstone disease, AJR Am. J. Roentgenol. 206 (1) (2016) 74–80.
[21] J.W. Uyeda, I.J. Richardson, A.D. Sodickson, Making the invisible visible: improving conspicuity of noncalcified gallstones using dual-energy CT, Abdom. Radiol. (NY) 42 (12) (2017) 2933–2939.
[22] C.B. Yang, S. Zhang, Y.J. Jia, H.F. Duan, G.M. Ma, X.R. Zhang, Y. Yu, T.P. He, Clinical application of dual-energy spectral computed tomography in detecting cholesterol gallstones from surrounding bile, Acad. Radiol. 24 (4) (2017) 478–482.
[23] H. Saito, K. Noda, K. Ogasawara, S. Atsuji, H. Takaoka, H. Kajihara, J. Nasu, S. Morishita, I. Matsushita, K. Katahira, Usefulness and limitations of dual-layer spectral detector computed tomography for diagnosing biliary stones not detected by conventional computed tomography: a report of three cases, Clin. J. Gastroenterol. 11 (2) (2018) 172–177.
[24] L. Ratanaprasatporn, J.W. Uyeda, J.R. Wortman, I. Richardson, A.D. Sodickson, Multimodality imaging, including dual-energy CT, in the evaluation of gallbladder disease, Radiographics 38 (1) (2018) 75–89.
[25] D. Marin, D.T. Boll, A. Mileto, R.C. Nelson, State of the art: dual-energy CT of the abdomen, Radiology 271 (2) (2014) 327–342.
[26] A. Graser, T.R. Johnson, E.M. Hecht, C.R. Becker, C. Leidecker, M. Staehler, C.G. Stief, H. Hildebrandt, M.C. Godoy, M.E. Finn, F. Stepansky, M.F. Reiser, M. Macari, Dual-energy CT in patients suspected of having renal masses: can virtual nonenhanced images replace true nonenhanced images? Radiology 252 (2) (2009) 433–440.
[27] C.N. De Cecco, A. Darnell, N. Macias, J.R. Ayuso, S. Rodriguez, J. Rimola, M. Pages, A. Garcia-Criado, M. Rengo, A. Laghi, C. Ayuso, Virtual unenhanced images of the abdomen with second-generation dual-source dual-energy computed tomography: image quality and liver lesion detection, Invest. Radiol. 48 (1) (2013) 1–9.
[28] The 2007 recommendations of the international commission on radiological protection. ICRP publication 103, Ann. ICRP 37 (2-4) (2007) 1–332.
[29] F.H. Miller, C.M. Hwang, H. Gabriel, L.A. Goodhartz, A.J. Omar, W.G. Parsons 3rd, Contrast-enhanced helical CT of choledocholithiasis, AJR Am. J. Roentgenol. 181 (1) (2003) 125–130.
[30] W.C. Chan, B.N. Joe, F.V. Coakley, E.L. Prien Jr., R.G. Gould, S. Prevrhal, W.C. Barber, K.S. Kirkwood, A. Qayyum, B.M. Yeh, Gallstone detection at CT in vitro: effect of peak voltage setting, Radiology 241 (2) (2006) 546–553.